

# A benchmark study of dioxygen complexes based on coupled cluster and density functional theory

Marcel Swart<sup>1,2,\*</sup>, Marc Reimann<sup>3</sup>

<sup>1</sup> ICREA, Pg. Lluís Companys 23, 08010 Barcelona, Spain

<sup>2</sup> IQCC and Dept. Chem., Univ. Girona, c/M. A. Capmany 69, 17003 Girona, Spain

<sup>3</sup> Institut für Chemie, Theoretische Chemie/Quantenchemie, Technische Universität Berlin, Sekr. C7, Straße des 17. Juni 135, D-10623 Berlin, Germany

\* [marcel.swart@icrea.cat](mailto:marcel.swart@icrea.cat)

## Abstract

A set of five compounds containing peroxy, superoxy or bis- $\mu$ -oxo moieties has been studied in the gas phase using CCSD(T)/aug-cc-pVQZ, also in combination with Goodson's continued fraction approach. The corresponding analytical frequencies corroborate assignments of bands from experiments, and thus provide a consistent set of reference data that can be used for benchmarking a range of density functional approximations. A total of 100 density functionals have been checked for the general bond lengths, the specific peroxy/superoxy bond lengths, angles, and vibrational frequencies. There is not one density functional that performs equally well for all of these properties, not even within one class of density functionals.



Copyright M. Swart and M. Reimann.  
This work is licensed under the Creative Commons  
[Attribution 4.0 International License](https://creativecommons.org/licenses/by/4.0/).  
Published by the SciPost Foundation.

Received 16-08-2023

Accepted 23-07-2024

Published 13-08-2024

doi:[10.21468/SciPostChem.3.1.001](https://doi.org/10.21468/SciPostChem.3.1.001)



Check for  
updates

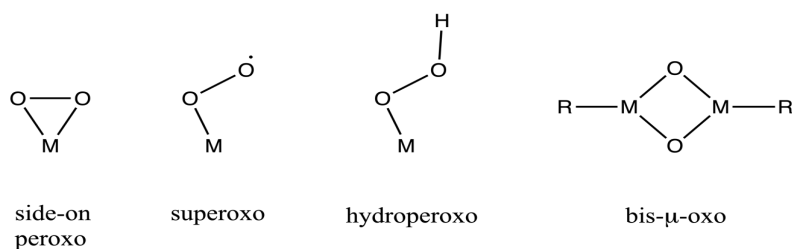
---

## Contents

<b>1 Introduction</b>	<b>2</b>
<b>2 Results and Discussion</b>	<b>3</b>
<b>3 Conclusions</b>	<b>10</b>
<b>4 Computational details</b>	<b>10</b>
<b>Acknowledgements</b>	<b>12</b>
<b>References</b>	<b>12</b>

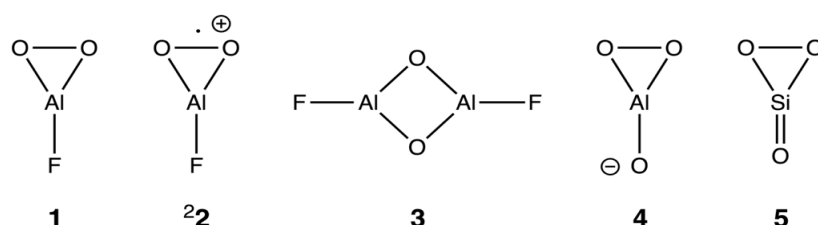
## 1 Introduction

Dioxygen can coordinate to first-row transition metals (in different oxidation and spin states) with several protonation states, and hapticity, leading to e.g. peroxo, superoxo, hydroperoxo or bis- $\mu$ -oxo species (see Scheme 1). Although crystal structures exist for all of these species [1,2], the corresponding complexes are too large for treatment by accurate wavefunction methods like CCSD(T) with large basis sets (aug-cc-pVQZ or better). This prevents the systematic validation [3-8] of more efficient yet less accurate quantum-chemistry methods, e.g. based on density functional theory [9], leading to uncertainty about the reliability and appropriateness of different density functionals [10,11] for this metal-dioxygen chemistry.



Scheme 1: Typical coordination of dioxygen towards (transition-)metal centers.

Fortunately, in the early 2000s a series of papers by Schnöckel [12,13] and co-workers reported the detection of peroxo and bis- $\mu$ -oxo complexes of aluminium (see Scheme 2), with vibrational spectroscopic data available for characterization. Furthermore, Tremblay and Roy characterized silicon trioxide compounds spectroscopically [14]. Since these complexes are small (maximum six atoms), and highly symmetric, it is possible to study them by high-level wavefunction methods with sufficiently large basis sets. Hence, here we used CCSD(T) [15] with the aug-cc-pVQZ (and aug-cc-pV(X+d)Z [16], X=T,Q) basis sets for complexes 1-5 (Scheme 2) to optimize their structure and compute the corresponding vibrational frequencies. Because of the well-known instability of coupled cluster frequencies for close-lying electronic states, in particular when using unrestricted Hartree-Fock (HF) orbitals [17], we have complemented these data with CCSD(T) results based on restricted open-shell Kohn-Sham (ROKS) PBE orbitals, and CASPT2 frequencies. These results match the standard CCSD(T) results very well, when the underlying HF solution exhibits no close-lying electronic states. These data can then serve as reference data for the development of new density functionals. Here, the results were used as reference data for the benchmarking of density functional approximations, to explore how well the latter reproduce the metal-O and O-O distances, the angles, and the vibrational frequencies.



Scheme 2: Al/Si complexes studied in this paper (complex 2 has overall charge +1, complex 4 overall charge -1, the other three are charge neutral). Experimental vibrational spectra are available for 1 [12], 3 [13], and for 5 [14].

## 2 Results and Discussion

**Coupled cluster results.** The experimentally observed vibrational data [12-14] for **1**, **3**, **5** are reported in Table 1, together with the CCSD(T)/aug-cc-pVQZ values. Also included are two related compounds, **2** and **4**, for which only the coupled cluster data are available. For **1** and **2** we also report CASPT2 results based on a CASSCF(14,8) reference. In general, there is a very good agreement between the experimentally observed peaks and the coupled cluster data. For instance, for  $[\text{FAlO}_2]^0$  the peaks were observed experimentally at 1077 and 782  $\text{cm}^{-1}$ , which match the harmonic coupled cluster frequencies of 1102 and 797  $\text{cm}^{-1}$ ; note that the difference between experiment and theory (2-3%) is due to anharmonicity. We have computed the anharmonic CCSD(T) frequencies based on VPT2, which shows a very good match of the effect of anharmonicity on these frequencies (see Table 2). The only exception perhaps may be the 1015  $\text{cm}^{-1}$  band of **3**, which after anharmonic corrections is observed at 995  $\text{cm}^{-1}$  with CCSD(T).

Few of the computed frequencies were observed experimentally, either due to too low intensity or not being able to assign these specifically to one of the manifolds of possible compounds that might be present in the experiments. For instance, in the reaction of AlF with  $\text{O}_2$  the authors observed (at least) three species: **1**, **3** and a third one involving four oxygens (assigned [12] as a di-superoxo species  $[\text{FAl}(\text{O}_2^{\cdot -})_2]^0$ ). Based on isotope effects when treating all species with either  $^{16}\text{O}_2$ ,  $^{18}\text{O}_2$  or a mixture of these, they were able to assign most of the observed peaks to one of these three species.

Table 1: Vibrational data ( $\text{cm}^{-1}$ ) for dioxygen complexes<sup>a</sup> (harmonic frequencies for CCSD(T)).

<b>1</b>		<b>2</b>		<b>3</b>		<b>4</b>		<b>5</b>	
exp. <sup>b</sup>	CCSD(T) <sup>c</sup>	CCSD(T) <sup>d</sup>	exp. <sup>e</sup>	CCSD(T) <sup>c</sup>	CCSD(T) <sup>c</sup>	exp. <sup>f</sup>	CCSD(T) <sup>c</sup>	CCSD(T) <sup>c</sup>	CCSD(T) <sup>c</sup>
1077.3	1102.3 (160.6)	1111.0	1015.0	1014.5 (0.0)	1100.4 (82.8)	1363.5	1382.2 (121.2)		
781.8	797.1 (26.7)	1001.4	942.8	966.1 (544.4)	748.1 (25.5)	877.1	887.6 (5.0)		
-	720.5 (8.8)	609.8	812.9	821.4 (312.4)	673.3 (27.2)	855.3	860.4 (17.5)		
-	476.0 (13.0)	596.1	-	749.3 (0.0)	544.0 (51.0)	-	511.3 (16.9)		
-	228.5 (122.1)	173.2	-	690.5 (0.0)	270.1 (33.2)	292.0	307.2 (80.7)		
-	219.8 (71.5)	172.8	-	665.1 (32.1)	256.8 (11.9)	287.8	296.4 (53.0)		
			-	404.5 (0.0)					
			-	400.7 (184.6)					
			-	243.7 (0.0)					
			-	225.2 (0.0)					
			-	171.1 (30.5)					
			-	94.5 (12.6)					

a) shown in (parentheses) are the computed IR intensities ( $\text{km} \cdot \text{mol}^{-1}$ ); b) [12]; c) CCSD(T)/aug-cc-pVQZ; d) ROKS-CCSD(T)/aug-cc-pVQZ on PBE orbitals; e) [13]; f) [14].

The normal modes for  $[\text{FAlO}_2]^0$  from CCSD(T)/aug-cc-pVQZ consist of an Al-F stretch at  $1102\text{ cm}^{-1}$ , the anti-symmetric ( $797\text{ cm}^{-1}$ ) and symmetric ( $721\text{ cm}^{-1}$ ) Al-O<sub>2</sub> vibrations, the O-O vibration ( $476\text{ cm}^{-1}$ ) and the out-of-plane ( $\delta$ -oop,  $229\text{ cm}^{-1}$ ) and in-plane ( $\delta$ -ip,  $220\text{ cm}^{-1}$ )  $\delta(\text{FAlOO})$  distortion. Similar modes are found for  $[\text{OAlO}_2]^0$ :  $\nu(\text{Al-O})$   $1100\text{ cm}^{-1}$ ,  $\nu_{\text{sym}}(\text{Al-O}_2)$   $748\text{ cm}^{-1}$ ,  $\nu_{\text{asym}}(\text{Al-O}_2)$   $673\text{ cm}^{-1}$ ,  $\nu(\text{O-O})$   $544\text{ cm}^{-1}$ ,  $\nu(\delta\text{-oop})$   $270\text{ cm}^{-1}$ ,  $\nu(\delta\text{-ip})$   $257\text{ cm}^{-1}$ , and for  $[\text{OSi}(\text{O}_2)]^0$ :  $\nu(\text{Si-O})$   $1382\text{ cm}^{-1}$ ,  $\nu_{\text{sym}}(\text{Si-O}_2)$   $888\text{ cm}^{-1}$ ,  $\nu_{\text{asym}}(\text{Si-O}_2)$   $860\text{ cm}^{-1}$ ,  $\nu(\text{O-O})$   $511\text{ cm}^{-1}$ ,  $\nu(\delta\text{-oop})$   $307\text{ cm}^{-1}$ ,  $\nu(\delta\text{-ip})$   $296\text{ cm}^{-1}$ . Note that in these latter cases the symmetric Al/Si-O<sub>2</sub> stretch shows a higher frequency than the asymmetric stretch, unlike the case of  $[\text{FAlO}_2]^0$ . Instead, for  ${}^2[\text{FAlO}_2]^{*+}$  the normal modes are shifted drastically in some cases:  $\nu(\text{Al-F})$   $1111\text{ cm}^{-1}$ ,  $\nu(\text{O-O})$   $1001\text{ cm}^{-1}$ ,  $\nu_{\text{sym}}(\text{Al-O}_2)$   $610\text{ cm}^{-1}$ ,  $\nu_{\text{asym}}(\text{Al-O}_2)$   $596\text{ cm}^{-1}$ ,  $\nu(\delta\text{-oop})$   $173\text{ cm}^{-1}$ ,  $\nu(\delta\text{-ip})$   $173\text{ cm}^{-1}$ . These calculations, however, had to be performed using PBE-based orbitals, as the usage of HF based orbitals resulted in unphysically large shifts. This approach is well suited as it introduces only marginal deviations from HF-based results for all other species (see Table S7). Finally, for  $[\text{FAl}(\mu\text{-O})_2\text{AlF}]^0$  the Al-F stretches are found at  $1015\text{ cm}^{-1}$  (sym) and  $966\text{ cm}^{-1}$  (asym), the Al-O<sub>2</sub>-Al stretches at  $691\text{ cm}^{-1}$  (asym) and  $665\text{ cm}^{-1}$  (sym), and further modes involving the diamond-core breathing mode ( $749\text{ cm}^{-1}$ ), FAl-AlF stretch ( $405\text{ cm}^{-1}$ ), in-plane Al<sub>2</sub> vs. O<sub>2</sub> ( $821\text{ cm}^{-1}$ ), out-of-plane Al<sub>2</sub> vs. O<sub>2</sub> ( $401\text{ cm}^{-1}$ ), rocking ( $244\text{ cm}^{-1}$ ) vs. flying ( $171\text{ cm}^{-1}$ ) vs. out-of-plane ( $95\text{ cm}^{-1}$ ) motions of Al<sub>2</sub>O<sub>2</sub> vs. F<sub>2</sub>, and the anti-symmetric out-of-plane wobble of Al<sub>2</sub>F<sub>2</sub> ( $225\text{ cm}^{-1}$ ). Note that gif-movie files for all modes are available in Supporting Information.

Table 2: Effect of anharmonicity on computed vibrational data ( $\text{cm}^{-1}$ ) for dioxygen complexes<sup>a</sup>.

<b>1</b>			<b>3</b>			<b>5</b>		
exp. <sup>b</sup>	harm.	anharm.	exp. <sup>c</sup>	harm.	anharm.	exp. <sup>d</sup>	harm.	anharm.
1077.3	1093.7	1078.3	1015.0	1007.0	994.7	1363.5	1384.7	1364.4
781.8	790.9	781.2	942.8	958.1	943.8	877.1	890.1	877.9
-	716.6	707.3	812.9	816.9	805.9	855.3	863.3	851.9
-	476.8	463.1	-	747.0	738.5	-	513.1	496.1
-	232.8	233.0	-	684.9	673.2	292.0	304.5	303.4
-	219.3	219.5	-	660.2	657.1	287.8	296.5	295.1
				404.5	399.7			
				399.9	397.6			
				245.8	245.2			
				229.4	229.5			
				173.7	173.7			
				98.1	98.3			

a) data obtained at CCSD(T)/def2-tzvpd; b) [12]; c) [13] d) [14].

The geometric variables (bonds, angles) from the coupled cluster calculations are reported in Table 3. Based on the revised covalent radii by Alvarez and co-workers from 2008 [18], one would expect Al-F bonds of  $1.78\text{ \AA}$ , Al-O bonds of  $1.87\text{ \AA}$ , and Si-O

bonds of 1.77 Å. Here, we observe Al-F, Al-O and Si-O bonds that are significantly shorter (0.15-0.20 Å). However, they are consistent with previous computational studies at lower levels of theory [13,19,20]. Furthermore, the coupled cluster method with such a large basis set is often considered the ‘gold standard’ of computational chemistry. Indeed, the strong coherence between the computed and observed IR frequencies reinforce this notion. For this reason, the coupled cluster data provide a good reference set to be able to compare density functional approximations with.

Table 3: Geometric variables obtained at CCSD(T)/aug-cc-pVQZ (using ROKS orbitals for 2).

bond	(Å)	angle	(°)
<b>1</b>			
F-Al	1.62978	F-Al-O	150.286
Al-O(O <sub>2</sub> )	1.69710	O-Al-O <sup>a</sup>	59.428
O-O	1.68239		
<b>2</b>			
F-Al	1.59705	F-Al-O	156.951
Al-O(O <sub>2</sub> )	1.78213	O-Al-O <sup>a</sup>	46.098
O-O	1.39549		
<b>3</b>			
F-Al	1.63660	F-Al-O	133.328
Al-O	1.73798	Al-O-Al	86.655
Al-Al <sup>a</sup>	2.38510		
<b>4</b>			
O-Al	1.63751	O-Al-O	152.282
Al-O(O <sub>2</sub> )	1.74850	O-Al-O <sup>a</sup>	55.437
O-O	1.62655		
<b>5</b>			
O-Si	1.50991	O-Si-O(O <sub>2</sub> )	148.864
Si-O(O <sub>2</sub> )	1.62299	O(O <sub>2</sub> )-Si-O(O <sub>2</sub> ) <sup>a</sup>	62.271
O-O	1.67839		

a) not used for the deviations of density functional results (use of symmetry makes this value dependent on the other angle)

**Density functional results.** A total of 100 density functional approximations (DFAs) were tested against the coupled cluster reference data. Note that the same conditions were used as were employed for coupled cluster: using the aug-cc-pVQZ basis in the gas phase and without relativistic corrections. Hence, we looked at the bond lengths and angles (see Table 3), and frequencies.

There were four DFAs (PWPB95, mPWB1K, mPW1B95, PW6B95) that showed SCF problems during one or more of the optimizations and frequency calculations, which in all cases involved the <sup>2</sup>[FAlO<sub>2</sub>]<sup>++</sup> system. Additionally, mPW1B95 showed problems as well for [FAlO<sub>2</sub>]<sup>0</sup> and [FAl(μ-O)<sub>2</sub>AlF]<sup>0</sup>. These problems were likely caused by the well

known numerical instability of the B95 correlation functional [21], which was solved by increasing the integration grid to (770,123) for the singlet systems. Further modifications were needed for the unrestricted  $^2[\text{FAIO}_2]^{++}$  system: changing the SCF procedure to EDIIS and loosening the convergence criteria for energy ( $10^{-7}$  Hartree) and density ( $10^{-5}$  atomic units) solved the issues there as well.

The mean absolute deviation (MAD) from the coupled cluster reference data for *all* bonds (Table S1) is smallest for the B97-3c composite functional (MAD value 0.0056 Å), followed by MS1/MS2 metagga and the r2SCAN-3c composite functionals (MAD values 0.0064-0.0067 Å), followed by TPSS (0.0079 Å), the MGGA-hybrid TPSSh (0.0092 Å), revised TPSS (0.0092 Å) and the B97-D2 GGA (0.0094 Å). The best hybrid functional is B3LYP with a MAD value of 0.0118 Å, TMHF the best local hybrid functional (0.0156 Å), RC04 is the best LDA functional (0.0169 Å), HSE06 the best range-separated hybrid functional (0.0234 Å), wLH23tb the best range-separated local hybrid functional (0.0263 Å), and B2PLYP the best double-hybrid functional (0.0357 Å). The lower end of the table is filled with more exotic functionals like revSCAN0 or MVSh, but also includes double-hybrid functionals like DSD-PBEP86 (0.0484 Å) or DSD-BLYP (0.0497 Å).

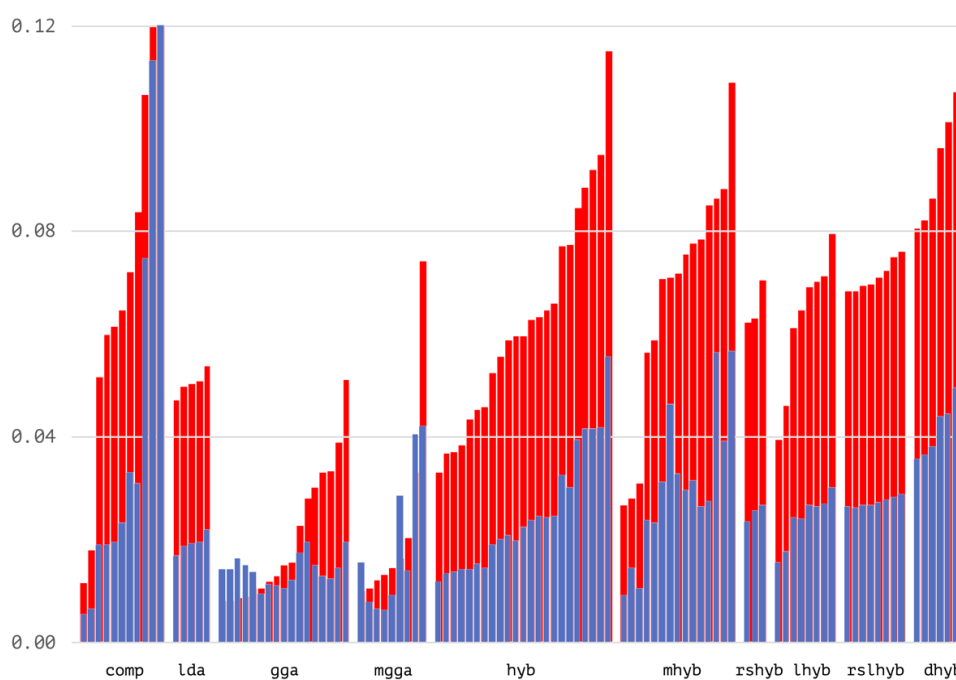


Figure 1: Mean absolute deviations (Å) of all bonds (blue, Table S1) and peroxy/superoxy-bonds alone (red, Table S2) for the 100 density functionals compared to the CCSD(T)/aug-cc-pVQZ reference data. Shown from left to right are the classes of composites, LDA, GGA, MGGA, hybrid, MGGA-hybrid, range-separated hybrid, local hybrid, range-separated local hybrid and double hybrid.

If we now specifically focus on the peroxy/superoxy O-O bonds alone (Table S2, Figure 1), a different picture emerges. TCA, revTCA, RPBE and revPBE are suddenly the best (0.0082-0.0090 Å), followed by PKZB (0.0099 Å), TPSS (0.0105 Å), the Chachiyo and

B97-D GGA (0.0106 Å) and B97-3c (0.0116 Å). The best MGGA-hybrid, hybrid, local hybrid, LDA, range-separated hybrid and range-separated local hybrid functionals are again TPSSH, B3LYP, TMHF, RC04, HSE06, and wLH23tb but with MAD values (0.0267 Å, 0.0330 Å, 0.0396 Å, 0.0472 Å, 0.0623 Å, and 0.0685 Å, respectively) that are more than twice as large as for all bonds. The same holds for B2PLYP, which remains the best-performing double-hybrid functional, but with a MAD value for the peroxy/superoxy bonds of 0.0806 Å. These problems for describing peroxy bonds is observed for many DFAs (see Figure 1).

Most of the density functionals are able to predict well the angles (Table S3), with MAD values of less than 1°, but now with other best-performing functionals for most of the classes: BLYP for GGAs (MAD 0.213°), M06-L for MGGAs (MAD 0.278°), r2SCAN-3c the best composite (MAD 0.302°); B3LYP and TMHF remain best hybrid and local hybrid functional (MAD 0.363° and 0.417°, respectively), MS2h is the best MGGA-hybrid functional (MAD 0.383°), CAM-B3LYP the best range-separated hybrid functional (MAD 0.687°), RC04 best LDA functional (MAD 0.705°), wLH23tp the best range-separated local hybrid (MAD 0.757°) and PTPSS the best double hybrid (MAD 0.851°).

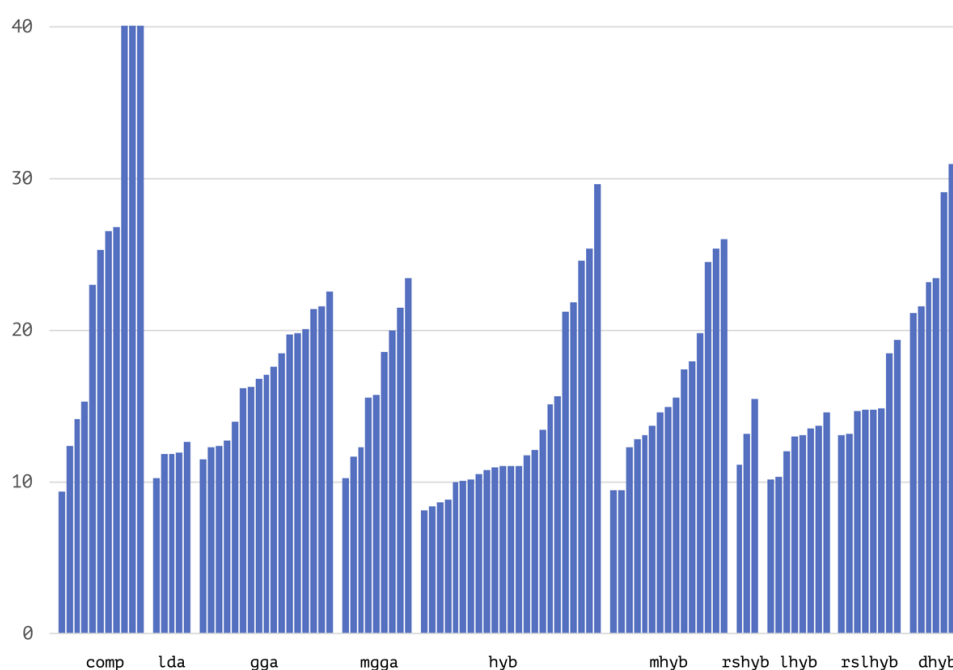


Figure 2. Mean absolute deviations ( $\text{cm}^{-1}$ ) of vibrational frequencies for the 100 density functionals compared to the CCSD(T)/aug-cc-pVQZ reference data. Shown from left to right are the classes of composites, LDA, GGA, MGGA, hybrid, MGGA-hybrid, range-separated hybrid, local hybrid, range-separated local hybrid and double hybrid.

The picture changes again completely when looking at the vibrational frequencies (Table S4, Figure 2). Note that the DFT frequencies were computed at the CCSD(T) geometries; this allows to separate clearly the effect of accuracy for geometries (Tables S1-S3) from the accuracy for frequencies (Table S4). Here the hybrid functionals in all

the different guises are observed at the upper half of the list, with the O3LYP hybrid functional performing best (MAD 8.1  $\text{cm}^{-1}$ ), followed closely by B97 (8.4  $\text{cm}^{-1}$ ), and B97-1 (8.7  $\text{cm}^{-1}$ ). The best composite is again r2SCAN-3c (9.4  $\text{cm}^{-1}$ ). The best MGGA-hybrid functional is now TPSSh (MAD 9.5  $\text{cm}^{-1}$ ), TMHF is the best local hybrid again (MAD 10.1  $\text{cm}^{-1}$ ), M06-L is the best metagga functional (MAD 10.2  $\text{cm}^{-1}$ ), RC04 the best LDA functional (10.3  $\text{cm}^{-1}$ ), HSE06 the best range-separated hybrid functional (MAD 11.1  $\text{cm}^{-1}$ ), OPBE the best GGA functional (MAD 11.5  $\text{cm}^{-1}$ ), wLH23tde the best range-separated local hybrid (MAD 13.1  $\text{cm}^{-1}$ ), and PWPB95 the best double-hybrid functional (MAD 21.2  $\text{cm}^{-1}$ ). Most of the list of 100 DFAs show MAD values for the vibrational frequencies that remain below 20  $\text{cm}^{-1}$ , and 68 are within 10  $\text{cm}^{-1}$  from the best performing one.

Overall assessment. Based on the MAD values for the four different properties (Table S1-S4), we also made an average assessment of the different density functionals. This was done by taking for each DFA the product of the MAD values for the different properties (PROD, shown in Table S5). The top 10 of this final list consists only of composite, GGA and MGGA functionals, with B97-3c at the top (PROD 0.00030  $\text{\AA}^2 \cdot \text{cm}^{-1}$ ), followed closely by MS2 and MS1 (PROD 0.00031  $\text{\AA}^2 \cdot \text{cm}^{-1}$ ), and r2SCAN-3c (PROD 0.00033  $\text{\AA}^2 \cdot \text{cm}^{-1}$ ). The best functionals for each class of DFAs are: B97-3c (composite, PROD 0.00030  $\text{\AA}^2 \cdot \text{cm}^{-1}$ ), MS2 (MGGA, PROD 0.00031  $\text{\AA}^2 \cdot \text{cm}^{-1}$ ), B97-D2 (GGA, PROD 0.00049  $\text{\AA}^2 \cdot \text{cm}^{-1}$ ), TPSSh (MGGA-hybrid, PROD 0.00093  $\text{\AA}^2 \cdot \text{cm}^{-1}$ ), B3LYP (hybrid, PROD 0.00142  $\text{\AA}^2 \cdot \text{cm}^{-1}$ ), TMHF (local hybrid, PROD 0.00262  $\text{\AA}^2 \cdot \text{cm}^{-1}$ ), RC04 (LDA, 0.00580  $\text{\AA}^2 \cdot \text{cm}^{-1}$ ), HSE06 (range-separated hybrid, PROD 0.01161  $\text{\AA}^2 \cdot \text{cm}^{-1}$ ), wLH23tB (range-separated local hybrid, PROD 0.02018  $\text{\AA}^2 \cdot \text{cm}^{-1}$ ), and PTPSS (double hybrid, PROD 0.05523  $\text{\AA}^2 \cdot \text{cm}^{-1}$ ).

The average PROD value for all 100 functionals is rather high (0.32  $\text{\AA}^2 \cdot \text{cm}^{-1}$ ), but this is distorted by the high value for HF-3c (2.477  $\text{\AA}^2 \cdot \text{cm}^{-1}$ ). Instead, by taking the product of the averages for each of the four properties (Table 4), one obtains a PROD value of only 0.025  $\text{\AA}^2 \cdot \text{cm}^{-1}$ , which is a more appropriate overall measure.

Table 4. Statistics for deviations by DFAs (Table S1-S5) from CCSD(T)/aug-cc-pVQZ data.

	min. MAD	max. MAD	average
all bonds ( $\text{\AA}$ )	0.0056	0.1303	0.0265
dioxygen bonds ( $\text{\AA}$ )	0.0083	0.2674	0.0591
angles ( $^\circ$ )	0.2125	3.1014	0.7677
frequencies ( $\text{cm}^{-1}$ )	8.133	262.430	20.956
product	0.000080	28.358097	0.025196



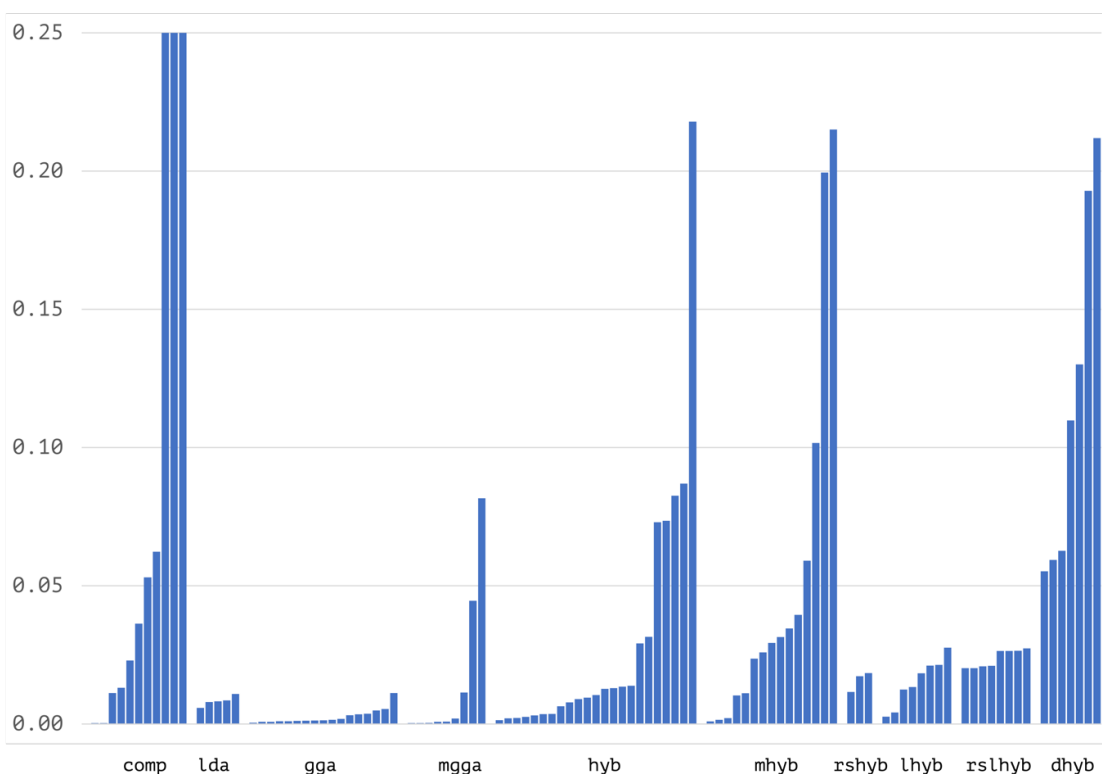


Figure 3. Overall assessment ( $\text{\AA}^2 \cdot ^\circ \cdot \text{cm}^{-1}$ ) for the 100 density functionals compared to the CCSD(T)/aug-cc-pVQZ reference data. Shown from left to right are the classes of composites, LDA, GGA, MGGA, hybrid, MGGA-hybrid, range-separated hybrid, local hybrid, range-separated local hybrid and double hybrid.

Balance of exchange and correlation parts. For the dioxygen bonds, there is not a clear trend on the importance of either exchange or correlation. For instance, when comparing the deviations for  $\text{O}_2$  distances by a variety of functionals based on the PBEc and Becke88x functionals, we observe a clear and large effect of the exchange part. Whereas PBE itself slightly underestimates the  $\text{O}_2$  bond lengths (as estimated by inspecting the MD value in Table 5), the revPBE and RPBE functionals largely improve upon this. These latter two DFAs modify the exchange part of PBE. Likewise, OPBE, S12g and PBE1PBE, which modify the PBEx in different ways, show a systematic underestimation of the  $\text{O}_2$  bonds by 0.030  $\text{\AA}$  (S12g) to 0.066  $\text{\AA}$  (PBE1PBE). This appears to indicate a major effect by the choice of exchange functional. However, by comparing the results of combining Becke88 exchange with different correlation functionals, similar effects are seen (ranging from -0.006 to +0.023  $\text{\AA}$ ). Hence, both parts of the DFA formulation play an important role.

Table 5. Statistics<sup>a</sup> (Å) for deviations for O<sub>2</sub> bonds by DFAs based on PBEc and Becke88 parts.

DFA	X	C	MAD	MD	Max	Min
PBE	PBE <sub>x</sub>	PBE <sub>c</sub>	0.0157	-0.0104	0.0106	-0.0221
revPBE	revPBE <sub>x</sub>	PBE <sub>c</sub>	0.0091	-0.0003	0.0172	-0.0100
RPBE	RPBE <sub>x</sub>	PBE <sub>c</sub>	0.0087	0.0030	0.0195	-0.0062
OPBE	Opt <sub>x</sub>	PBE <sub>c</sub>	0.0511	-0.0511	-0.0176	-0.0699
S12g	S12g <sub>x</sub>	PBE <sub>c</sub>	0.0302	-0.0302	-0.0066	-0.0419
PBE1PBE	25% HFX +	PBE <sub>c</sub>	0.0659	-0.0659	-0.0330	-0.0856
	75% PBE <sub>x</sub>					
BP86(PZ81)	Becke88	P86 + PZ81	0.0119	-0.0042	0.0153	-0.0154
BP86(VWN)	Becke88	P86 + VWN	0.0129	-0.0059	0.0140	-0.0172
BLYP	Becke88	LYP <sub>c</sub>	0.0229	0.0229	0.0325	0.0169

a) MAD: Mean Absolute Deviation, MD: Mean Deviation, Max: Maximum deviation, Min: Minimum Deviation

### 3 Conclusions

A new set of small dioxygen compounds is presented, for which high-level ab initio calculations were feasible at the CCSD(T)/aug-cc-pVQZ level. The resulting data could be used as reference in the development of new density functionals, or used to benchmark existing density functionals. The latter is done here, for a total of 100 density functionals coming from ten classes (LDA, GGA, MGGA, hybrid, MGGA hybrid, range-separated hybrid, local hybrid, range-separated local hybrid, double hybrid and composites). In general, the density functionals are remarkably accurate for bonds and angles, with average deviations of 0.027 Å for *all* bonds, 0.77° for angles; dioxygen bonds are more difficult to get right, with an average deviation from the coupled cluster of 0.058 Å, more than twice as large as the deviation for all bonds. The cause for this is difficult to pinpoint onto ingredients of DFAs or specific chemical bonding patterns. The frequencies from coupled cluster calculations are off by ca. 10-20 cm<sup>-1</sup>, where it should be noted that the well-known Hartree-Fock instability can significantly affect the frequency values for open-shell systems.

### 4 Computational details

Coupled cluster: All CCSD(T) calculations with the aug-cc-pVQZ [22,23] and aug-cc-pV(Q+d)Z [16] basis set were carried out with CFOUR (version 2.0/2.1) [24,25], based on analytical gradients and Hessians [26-28], in parallel where needed [29], using unrestricted Hartree-Fock for open-shell systems. Note that a bugfix (Dec. 2021, see SI) was needed for being able to run in parallel with unrestricted coupled cluster protocols.

Basis sets not available in standard CFOUR (e.g. def2-TZVPD or aug-cc-pV(Q+d)Z) were obtained from the basis set exchange [30]. The frozen core approach was used within the solving of the coupled cluster equations. The geometry optimization typically had SCF and coupled-cluster convergence criteria of  $1.0 \cdot 10^{-10}$ , geometry converge of  $1.0 \cdot 10^{-8}$  atomic units, leading to electronic energies accurate to at least  $1.0 \cdot 10^{-8}$  Hartree. The two-electron integrals were in all cases treated with the AOBASIS formalism to reduce disk space, in conjunction with the ECC program (with conventional UCCSD(T) for complex 2).

Additional CCSD(T) calculations using the same basis set and R(O)KS orbitals obtained by the PBE functional were performed with the MOLPRO program package (Version 2022.2) [31,32]. All calculations employed the spin-unrestricted CCSD(T) routines (UCCSD(T)) to correctly handle the KS orbitals.

At the same level, also CASPT2 calculations were performed using a CASSCF wave function based on an active space containing the 2s and 2p orbitals of both O atoms. The initial guess for the active space was obtained using the atomic valance active space (AVAS) procedure [33] based on R(O)HF orbitals and both CASSCF and CASPT2 employed density fitting [34].

Density functional theory: Most density functional calculations were calculated with the psi4 program (release 1.6.1, the composite results were obtained with version 1.9) [35-37]. For optimizations, the most tight criteria available in the program were used (*gradient max*  $2.0 \cdot 10^{-6}$  a.u., *RMS force*  $1.0 \cdot 10^{-6}$  a.u., *max displacement*  $6.0 \cdot 10^{-6}$  a.u., *rms displacement*  $4.0 \cdot 10^{-6}$  a.u.), with typically a grid based on 590 spherical points and 99 radial points. The doublet states (2) were treated using the unrestricted Kohn-Sham formalism. Similar to coupled cluster, the DFA calculations were performed in the gas-phase, without relativistic corrections, and using the aug-cc-pVQZ basis set (using RI/DF basis sets, AUG-CC-PVQZ AUX). Some of the results for density functional approximations were obtained through the LibXC [38] library, either the one available directly in psi4, or compiled separately and linked to it. We have studied DFAs of different classes: local density approximation (VWN(RPA) [39], VWN5 [39] and PW92 [40]), generalized gradient approximations (B97-d [41], BLYP [42,43], BP86-PZ81 [42,44,45], BP86-VWN [39,42,44], OPBE [46-48], PBE [48], PBEsol [49], PW91 [50], revPBE [51], RPBE [52], S12g [53], SOGGA [54], XLYP [55]), meta-GGA approximations (M06-L [56], MS1 [57], MS2 [57], MVS [58], PKZB [59], revSCAN [60], revTPSS [61], SCAN [62], TPSS [63]), hybrid functionals (B1LYP [64], B1PW91 [64], B3LYP [42,43,65], B3PW91 [42,50,66], B97 [67], B97-1 [68], B97-2 [69], B97-3 [70], B97-k [71], BHandH [42,66], BHandHLYP [42,43,66], HJS-PBE [72], LDA1LDA [73], mPW1K [74], mPW1PW [75], mPWB1K [76], O3LYP [43,47,77], PBE1PBE [48,78], revB3LYP [79], revPBE1PBE [48,51,78], SOGGA11-X [80], X3LYP [55]), hybrid meta-GGA (BB1K [81], BMK [71], M06 [82], M06-2X [82], M08-HX [83], M11 [84], MS2h [57], MVSh [58], MN15 [85], mPW1B95 [76], PW6B95 [86], revSCAN1SCAN [60], revTPSSh [87], SCAN1SCAN [88], TPSSh [63,89]), range-separated hybrids (CAM-B3LYP [90], HSE06 [91-93], wB97X-D [94,95]), double hybrids (B2GPPLYP [96], B2PLYP [97], DSD-BLYP [98], DSD-PBEP86 [98], PBE1PBE-DH [99], PTPSS [100], PWPB95 [100]) and composite methods (HF-3c [101,102], PBEh-3c [101,102], B97-3c [103], r2SCAN-3c [104], wB97X-3c [105]). Note that wB97X-3c standard uses a vDZP basis set, which includes an Effective Core Potential (ECP); as a result the electronic energies are completely off (see Supporting Information). Therefore, similar to PBEh-3c the def2-mSVP basis has been used with

wB97X-3c; this change hardly affects angles and frequencies, slightly improves bonds, and has a major effect only on the electronic energy MAD (see SI).

Additional density functional calculations were performed using a development version of the TURBOMOLE program package based on version 7.8 [106,107]. The calculations employed basis sets and convergence criteria identical to those above and were performed using the “reference” grid settings based on 1202 spherical points and 90 radial points (95 for Al). Using TURBOMOLE, we evaluated functionals from additional classes: local hybrids (LH20t [108], LH23pt [109], TMHF [110], TMHF-3P [110], LHJ-HF [110], LHJ-HFcal [110], scLH22t [111], scLH23t-mBR [112]) and range-separated local hybrids (wLH22t [113], wLH23td [114], wLH23tE [114], wLH23tdE [114], wLH23tP [114], wLH23tdP [114], wLH23tB [114], wLH23tdB [114]).

## Acknowledgements

**Funding information.** The authors would like to thank AEI/MCIN (CTQ2017-87392-P, PID2020-114548GB-I00) and GenCat (2021 SGR 00487) for funding.

## References

- [1] C. J. Cramer, W. B. Tolman, K. H. Theopold and A. L. Rheingold, *Variable character of O-O and M-O bonding in side-on*, Proc. Natl. Acad. Sci. **100**, 3635 (2003), doi:[10.1073/pnas.0535926100](https://doi.org/10.1073/pnas.0535926100).
- [2] M. Swart, *A change in the oxidation state of iron: scandium is not innocent*, Chem. Commun. **49**, 6650 (2013), doi:[10.1039/c3cc42200c](https://doi.org/10.1039/c3cc42200c).
- [3] R. J. Deeth, N. Fey *The performance of nonhybrid density functionals for calculating the structures and spin states of Fe(II) and Fe(III) complexes* J. Comput. Chem. **25**, 1840 (2004), doi:[10.1002/jcc.20101](https://doi.org/10.1002/jcc.20101).
- [4] T. Weymuth, E. P. A. Couzijn, P. Chen and M. Reiher, *New benchmark set of transition-metal coordination reactions for the assessment of density functionals*, J. Chem. Theory Comput. **10**, 3092 (2014), doi:[10.1021/ct500248h](https://doi.org/10.1021/ct500248h).
- [5] B. J. Houghton and R. J. Deeth, *Spin-state energetics of FeII complexes - The continuing voyage through the density functional minefield*, Eur. J. Inorg. Chem. **2014**, 4573 (2014), doi:[10.1002/ejic.201402253](https://doi.org/10.1002/ejic.201402253).
- [6] M. Reimann and M. Kaupp, *Spin-state splittings in 3d transition-metal complexes revisited: Benchmarking approximate methods for adiabatic spin-state energy differences in Fe(II) complexes*, J. Chem. Theory Comput. **18**, 7442 (2022), doi:[10.1021/acs.jctc.2c00924](https://doi.org/10.1021/acs.jctc.2c00924).

- [7] M. Reimann and M. Kaupp, *Spin-state splittings in 3d transition-metal complexes revisited: Toward a reliable theory benchmark*, J. Chem. Theory Comput. **19**, 97 (2022), doi:[10.1021/acs.jctc.2c00925](https://doi.org/10.1021/acs.jctc.2c00925).
- [8] V. Vennelakanti, M. G. Taylor, A. Nandy, C. Duan and H. J. Kulik, *Assessing the performance of approximate density functional theory on 95 experimentally characterized Fe(II) spin crossover complexes*, J. Chem. Phys. **159**, 024120 (2023), doi:[10.1063/5.0157187](https://doi.org/10.1063/5.0157187).
- [9] W. Koch, M. C. Holthausen *A chemist's guide to density functional theory*, Wiley, New Jersey, United States, ISBN 9783527303724 (2001), doi:[10.1002/3527600043](https://doi.org/10.1002/3527600043).
- [10] C. J. Cramer and D. G. Truhlar, *Density functional theory for transition metals and transition metal chemistry*, Phys. Chem. Chem. Phys. **11**, 10757 (2009), doi:[10.1039/B907148B](https://doi.org/10.1039/B907148B).
- [11] M. Bursch, J. Mewes, A. Hansen and S. Grimme, *Best-practice DFT protocols for basic molecular computational chemistry*, Angew. Chem. Int. Ed. **61**, e202205735 (2022), doi:[10.1002/anie.202205735](https://doi.org/10.1002/anie.202205735).
- [12] J. Bahlo, H.-J. Himmel and H. Schnöckel, *The first detection of peroxo and bis-superoxo complexes of aluminum:  $FAIO_2$  and  $FAIO_4$* , Angew. Chem. Int. Ed. **40**, 4696 (2001), doi:[10.1002/1521-3773\(20011217\)40:24<4696::AID-ANIE4696>3.0.CO;2-W](https://doi.org/10.1002/1521-3773(20011217)40:24<4696::AID-ANIE4696>3.0.CO;2-W).
- [13] J. Bahlo, H.-J. Himmel and H. Schnöckel, *Photolytic reactions of subvalent aluminum(I) halides in the presence of dioxygen: Generation and characterization of the peroxo species  $XAlO_2$  and  $XAl(\mu-O)_2AlX$  ( $X = F, Cl, Br$ )*, Inorg. Chem. **41**, 2678 (2002), doi:[10.1021/ic011313d](https://doi.org/10.1021/ic011313d).
- [14] B. Tremblay, P. Roy, L. Manceron, M. E. Alikhani and D. Roy, *Vibrational spectrum and structure of silicon trioxide  $SiO_3$ : A matrix isolation infrared and density functional theory study*, J. Chem. Phys. **104**, 2773 (1996), doi:[10.1063/1.471100](https://doi.org/10.1063/1.471100).
- [15] T. Helgaker, P. Jørgensen and J. Olsen, *Molecular electronic-structure theory*, Wiley, New Jersey, United States, ISBN 9780471967552 (2000), doi:[10.1002/9781119019572](https://doi.org/10.1002/9781119019572).
- [16] T. H. Dunning, K. A. Peterson and A. K. Wilson, *Gaussian basis sets for use in correlated molecular calculations. X. The atoms aluminum through argon revisited*, J. Chem. Phys. **114**, 9244 (2001), doi:[10.1063/1.1367373](https://doi.org/10.1063/1.1367373).
- [17] T. D. Crawford, J. F. Stanton, W. D. Allen and H. F. Schaefer, *Hartree-Fock orbital instability envelopes in highly correlated single-reference wave functions*, J. Chem. Phys. **107**, 10626 (1997), doi:[10.1063/1.474178](https://doi.org/10.1063/1.474178).

- [18] B. Cordero, V. Gómez, A. E. Platero-Prats, M. Revés, J. Echeverría, E. Cremades, F. Barragán and S. Alvarez, *Covalent radii revisited*, Dalton Trans. 2832 (2008), doi:[10.1039/B801115J](https://doi.org/10.1039/B801115J).
- [19] A. Hammerl, B. J. Welch and P. Schwerdtfeger, *F<sub>2</sub>Al(μ-η<sup>2</sup>:η<sup>2</sup>-O<sub>2</sub>)AlF<sub>2</sub>: An Unusual, Stable Aluminum Peroxo Compound*, Inorg. Chem. **43**, 1436 (2004), doi:[10.1021/ic035014v](https://doi.org/10.1021/ic035014v).
- [20] J. Bahlo, H.-J. Himmel and H. Schnöckel, *Characterization of the Side-On Coordinated Bissuperoxo Complexes of Aluminum FAl(O<sub>2</sub>)<sub>2</sub>, ClAl(O<sub>2</sub>)<sub>2</sub>, and BrAl(O<sub>2</sub>)<sub>2</sub> with Triplet Electronic Ground States: A Combined Matrix IR and Quantum Chemical Study*, Inorg. Chem. **41**, 4488 (2002), doi:[10.1021/ic020208g](https://doi.org/10.1021/ic020208g).
- [21] Y. Zhao and D. G. Truhlar, *Benchmark databases for nonbonded interactions and their use to test density functional theory*, J. Chem. Theory Comput. **1**, 415 (2005), doi:[10.1021/ct049851d](https://doi.org/10.1021/ct049851d).
- [22] R. A. Kendall, T. H. Dunning and R. J. Harrison, *Electron affinities of the first-row atoms revisited. Systematic basis sets and wave functions*, J. Chem. Phys. **96**, 6796 (1992), doi:[10.1063/1.462569](https://doi.org/10.1063/1.462569).
- [23] D. E. Woon and T. H. Dunning, *Gaussian basis sets for use in correlated molecular calculations. III. The atoms aluminum through argon*, J. Chem. Phys. **98**, 1358 (1993), doi:[10.1063/1.464303](https://doi.org/10.1063/1.464303).
- [24] Stanton, J. F., Gauss, J., Cheng, L., Harding, M. E., Matthews, D. A., Szalay, P. G. CFOUR, *Coupled-cluster techniques for computational chemistry, a quantum-chemical program package*.
- [25] D. A. Matthews, L. Cheng, M. E. Harding, F. Lipparini, S. Stopkowicz, T.-C. Jagau, P. G. Szalay, J. Gauss and J. F. Stanton, *Coupled-cluster techniques for computational chemistry: The CFOUR program package*, J. Chem. Phys. **152**, 214108 (2020), doi:[10.1063/5.0004837](https://doi.org/10.1063/5.0004837).
- [26] J. D. Watts, J. Gauss and R. J. Bartlett, *Open-shell analytical energy gradients for triple excitation many-body, coupled-cluster methods: MBPT(4), CCSD+T(CCSD), CCSD(T), and QCISD(T)*, Chem. Phys. Lett. **200**, 1 (1992), doi:[10.1016/0009-2614\(92\)87036-0](https://doi.org/10.1016/0009-2614(92)87036-0).
- [27] J. Gauss and J. F. Stanton, *Analytic CCSD(T) second derivatives*, Chem. Phys. Lett. **276**, 70 (1997), doi:[10.1016/S0009-2614\(97\)88036-0](https://doi.org/10.1016/S0009-2614(97)88036-0).
- [28] P. G. Szalay, J. Gauss and J. F. Stanton, *Analytic UHF-CCSD(T) second derivatives: implementation and application to the calculation of the vibration-rotation interaction constants of NCO and NCS*, Theor. Chem. Acc.: Theory Comput. Model. (Theor. Chim. Acta) **100**, 5 (1998), doi:[10.1007/s002140050360](https://doi.org/10.1007/s002140050360).

- [29] M. E. Harding, T. Metzroth, J. Gauss and A. A. Auer, *Parallel Calculation of CCSD and CCSD(T) analytic first and second derivatives*, J. Chem. Theory Comput. **4**, 64 (2007), doi:[10.1021/ct700152c](https://doi.org/10.1021/ct700152c).
- [30] B. P. Pritchard, D. Altarawy, B. Didier, T. D. Gibson and T. L. Windus, *New basis set exchange: An open, up-to-date resource for the molecular sciences community*, J. Chem. Inf. Model. **59**, 4814 (2019), doi:[10.1021/acs.jcim.9b00725](https://doi.org/10.1021/acs.jcim.9b00725).
- [31] H.-J. Werner et al., *The Molpro quantum chemistry package*, J. Chem. Phys. **152**, 144107 (2020), doi:[10.1063/5.0005081](https://doi.org/10.1063/5.0005081).
- [32] H.-J. Werner et al., *MOLPRO, Version 2022.2, a package of ab initio programs*, <https://www.molpro.net>.
- [33] E. R. Sayfutyarova, Q. Sun, G. K.-L. Chan and G. Knizia, *Automated construction of molecular active spaces from atomic valence orbitals*, J. Chem. Theory Comput. **13**, 4063 (2017), doi:[10.1021/acs.jctc.7b00128](https://doi.org/10.1021/acs.jctc.7b00128).
- [34] W. Győrffy, T. Shiozaki, G. Knizia and H.-J. Werner, *Analytical energy gradients for second-order multireference perturbation theory using density fitting*, J. Chem. Phys. **138**, 104104 (2013), doi:[10.1063/1.4793737](https://doi.org/10.1063/1.4793737).
- [35] D. G. A. Smith et al., *PSI4 1.4: Open-source software for high-throughput quantum chemistry*, J. Chem. Phys. **152**, 184108 (2020), doi:[10.1063/5.0006002](https://doi.org/10.1063/5.0006002).
- [36] J. Almlöf, K. Faegri and K. Korsell, *Principles for a direct SCF approach to LIAO-MOab-initio calculations*, J. Comput. Chem. **3**, 385 (1982), doi:[10.1002/jcc.540030314](https://doi.org/10.1002/jcc.540030314).
- [37] J. H. Van Lenthe, R. Zwaans, H. J. J. Van Dam and M. F. Guest, *Starting SCF calculations by superposition of atomic densities*, J. Comput. Chem. **27**, 926 (2006), doi:[10.1002/jcc.20393](https://doi.org/10.1002/jcc.20393).
- [38] S. Lehtola, C. Steigemann, M. J.T. Oliveira and M. A.L. Marques, *Recent developments in libxc — A comprehensive library of functionals for density functional theory*, SoftwareX **7**, 1 (2018), doi:[10.1016/j.softx.2017.11.002](https://doi.org/10.1016/j.softx.2017.11.002).
- [39] S. H. Vosko, L. Wilk and M. Nusair, *Accurate spin-dependent electron liquid correlation energies for local spin density calculations: a critical analysis*, Can. J. Phys. **58**, 1200 (1980), doi:[10.1139/p80-159](https://doi.org/10.1139/p80-159).
- [40] J. P. Perdew and Y. Wang, *Accurate and simple analytic representation of the electron-gas correlation energy*, Phys. Rev. B **45**, 13244 (1992), doi:[10.1103/PhysRevB.45.13244](https://doi.org/10.1103/PhysRevB.45.13244).

- [41] S. Grimme, *Semiempirical GGA-type density functional constructed with a long-range dispersion correction*, J. Comput. Chem. **27**, 1787 (2006), doi:[10.1002/jcc.20495](https://doi.org/10.1002/jcc.20495).
- [42] A. D. Becke, *Density-functional exchange-energy approximation with correct asymptotic behavior*, Phys. Rev. A **38**, 3098 (1988), doi:[10.1103/physreva.38.3098](https://doi.org/10.1103/physreva.38.3098).
- [43] C. Lee, W. Yang and R. G. Parr, *Development of the Colle-Salvetti correlation-energy formula into a functional of the electron density*, Phys. Rev. B **37**, 785 (1988), doi:[10.1103/PhysRevB.37.785](https://doi.org/10.1103/PhysRevB.37.785).
- [44] J. P. Perdew, *Density-functional approximation for the correlation energy of the inhomogeneous electron gas*, Phys. Rev. B **33**, 8822 (1986), doi:[10.1103/PhysRevB.33.8822](https://doi.org/10.1103/PhysRevB.33.8822).
- [45] J. P. Perdew and A. Zunger, *Self-interaction correction to density-functional approximations for many-electron systems*, Phys. Rev. B **23**, 5048 (1981), doi:[10.1103/PhysRevB.23.5048](https://doi.org/10.1103/PhysRevB.23.5048).
- [46] M. Swart, A. W. Ehlers and K. Lammertsma, *Performance of the OPBE exchange-correlation functional*, Mol. Phys. **102**, 2467 (2004), doi:[10.1080/0026897042000275017](https://doi.org/10.1080/0026897042000275017).
- [47] N. C. Handy and A. J. Cohen, *Left-right correlation energy*, Mol. Phys. **99**, 403 (2001), doi:[10.1080/00268970010018431](https://doi.org/10.1080/00268970010018431).
- [48] J. P. Perdew, K. Burke and M. Ernzerhof, *Generalized gradient approximation made simple*, Phys. Rev. Lett. **77**, 3865 (1996), doi:[10.1103/PhysRevLett.77.3865](https://doi.org/10.1103/PhysRevLett.77.3865).
- [49] J. P. Perdew, A. Ruzsinszky, G. I. Csonka, O. A. Vydrov, G. E. Scuseria, L. A. Constantin, X. Zhou and K. Burke, *Restoring the density-gradient expansion for exchange in solids and surfaces*, Phys. Rev. Lett. **100**, 136406 (2008), doi:[10.1103/PhysRevLett.100.136406](https://doi.org/10.1103/PhysRevLett.100.136406).
- [50] J. P. Perdew, J. A. Chevary, S. H. Vosko, K. A. Jackson, M. R. Pederson, D. J. Singh and C. Fiolhais, *Atoms, molecules, solids, and surfaces: Applications of the generalized gradient approximation for exchange and correlation*, Phys. Rev. B **46**, 6671 (1992), doi:[10.1103/PhysRevB.46.6671](https://doi.org/10.1103/PhysRevB.46.6671).
- [51] Y. Zhang and W. Yang, *Comment on "Generalized gradient approximation made simple"*, Phys. Rev. Lett. **80**, 890 (1998), doi:[10.1103/PhysRevLett.80.890](https://doi.org/10.1103/PhysRevLett.80.890).
- [52] B. Hammer, L. B. Hansen and J. K. Nørskov, *Improved adsorption energetics within density-functional theory using revised Perdew-Burke-Ernzerhof functionals*, Phys. Rev. B **59**, 7413 (1999), doi:[10.1103/PhysRevB.59.7413](https://doi.org/10.1103/PhysRevB.59.7413).



- [53] M. Swart, *A new family of hybrid density functionals*, Chem. Phys. Lett. **580**, 166 (2013), doi:[10.1016/j.cplett.2013.06.045](https://doi.org/10.1016/j.cplett.2013.06.045).
- [54] Y. Zhao and D. G. Truhlar, *Construction of a generalized gradient approximation by restoring the density-gradient expansion and enforcing a tight Lieb-Oxford bound*, J. Chem. Phys. **128**, 184109 (2008), doi:[10.1063/1.2912068](https://doi.org/10.1063/1.2912068).
- [55] X. Xu and W. A. Goddard, *The X3LYP extended density functional for accurate descriptions of nonbond interactions, spin states, and thermochemical properties*, Proc. Natl. Acad. Sci. **101**, 2673 (2004), doi:[10.1073/pnas.0308730100](https://doi.org/10.1073/pnas.0308730100).
- [56] Y. Zhao and D. G. Truhlar, *A new local density functional for main-group thermochemistry, transition metal bonding, thermochemical kinetics, and noncovalent interactions*, J. Chem. Phys. **125**, 194101 (2006), doi:[10.1063/1.2370993](https://doi.org/10.1063/1.2370993).
- [57] J. Sun, R. Haunschild, B. Xiao, I. W. Bulik, G. E. Scuseria and J. P. Perdew, *Semilocal and hybrid meta-generalized gradient approximations based on the understanding of the kinetic-energy-density dependence*, J. Chem. Phys. **138**, 044113 (2013), doi:[10.1063/1.4789414](https://doi.org/10.1063/1.4789414).
- [58] J. Sun, J. P. Perdew and A. Ruzsinszky, *Semilocal density functional obeying a strongly tightened bound for exchange*, Proc. Natl. Acad. Sci. **112**, 685 (2015), doi:[10.1073/pnas.1423145112](https://doi.org/10.1073/pnas.1423145112).
- [59] J. P. Perdew, S. Kurth, A. Zupan and P. Blaha, *Accurate density functional with correct formal properties: A step beyond the generalized gradient approximation*, Phys. Rev. Lett. **82**, 2544 (1999), doi:[10.1103/PhysRevLett.82.2544](https://doi.org/10.1103/PhysRevLett.82.2544).
- [60] P. D. Mezei, G. I. Csonka and M. Kállay, *Simple modifications of the SCAN meta-generalized gradient approximation functional*, J. Chem. Theory Comput. **14**, 2469 (2018), doi:[10.1021/acs.jctc.8b00072](https://doi.org/10.1021/acs.jctc.8b00072).
- [61] J. P. Perdew, A. Ruzsinszky, G. I. Csonka, L. A. Constantin and J. Sun, *Workhorse semilocal density functional for condensed matter physics and quantum chemistry*, Phys. Rev. Lett. **103**, 026403 (2009), doi:[10.1103/PhysRevLett.103.026403](https://doi.org/10.1103/PhysRevLett.103.026403).
- [62] J. Sun, A. Ruzsinszky and J. P. Perdew, *Strongly constrained and appropriately normed semilocal density functional*, Phys. Rev. Lett. **115**, 036402 (2015), doi:[10.1103/PhysRevLett.115.036402](https://doi.org/10.1103/PhysRevLett.115.036402).
- [63] J. Tao, J. P. Perdew, V. N. Staroverov and G. E. Scuseria, *Climbing the density functional ladder: Nonempirical meta-generalized gradient approximation designed for molecules and solids*, Phys. Rev. Lett. **91**, 146401 (2003), doi:[10.1103/PhysRevLett.91.146401](https://doi.org/10.1103/PhysRevLett.91.146401).

- [64] C. Adamo and V. Barone, *Toward reliable adiabatic connection models free from adjustable parameters*, Chem. Phys. Lett. **274**, 242 (1997), doi:[10.1016/S0009-2614\(97\)00651-9](https://doi.org/10.1016/S0009-2614(97)00651-9).
- [65] P. J. Stephens, F. J. Devlin, C. F. Chabalowski and M. J. Frisch, *Ab initio calculation of vibrational absorption and circular dichroism spectra using density functional force fields*, J. Phys. Chem. **98**, 11623 (1994), doi:[10.1021/j100096a001](https://doi.org/10.1021/j100096a001).
- [66] A. D. Becke, *Density-functional thermochemistry. III. The role of exact exchange*, J. Chem. Phys. **98**, 5648 (1993), doi:[10.1063/1.464913](https://doi.org/10.1063/1.464913).
- [67] A. D. Becke, *Density-functional thermochemistry. V. Systematic optimization of exchange-correlation functionals*, J. Chem. Phys. **107**, 8554 (1997), doi:[10.1063/1.475007](https://doi.org/10.1063/1.475007).
- [68] F. A. Hamprecht, A. J. Cohen, D. J. Tozer and N. C. Handy, *Development and assessment of new exchange-correlation functionals*, J. Chem. Phys. **109**, 6264 (1998), doi:[10.1063/1.477267](https://doi.org/10.1063/1.477267).
- [69] P. J. Wilson, T. J. Bradley and D. J. Tozer, *Hybrid exchange-correlation functional determined from thermochemical data and ab initio potentials*, J. Chem. Phys. **115**, 9233 (2001), doi:[10.1063/1.1412605](https://doi.org/10.1063/1.1412605).
- [70] T. W. Keal and D. J. Tozer, *Semiempirical hybrid functional with improved performance in an extensive chemical assessment*, J. Chem. Phys. **123**, 121103 (2005), doi:[10.1063/1.2061227](https://doi.org/10.1063/1.2061227).
- [71] A. D. Boese and J. M. L. Martin, *Development of density functionals for thermochemical kinetics*, J. Chem. Phys. **121**, 3405 (2004), doi:[10.1063/1.1774975](https://doi.org/10.1063/1.1774975).
- [72] T. M. Henderson, B. G. Janesko and G. E. Scuseria, *Generalized gradient approximation model exchange holes for range-separated hybrids*, J. Chem. Phys. **128**, 194105 (2008), doi:[10.1063/1.2921797](https://doi.org/10.1063/1.2921797).
- [73] P. Rinke, A. Schleife, E. Kioupakis, A. Janotti, C. Rödl, F. Bechstedt, M. Scheffler and C. G. Van de Walle, *First-principles optical spectra for F centers in MgO*, Phys. Rev. Lett. **108**, 126404 (2012), doi:[10.1103/PhysRevLett.108.126404](https://doi.org/10.1103/PhysRevLett.108.126404).
- [74] B. J. Lynch, P. L. Fast, M. Harris and D. G. Truhlar, *Adiabatic connection for kinetics*, J. Phys. Chem. A **104**, 4811 (2000), doi:[10.1021/jp000497z](https://doi.org/10.1021/jp000497z).
- [75] C. Adamo and V. Barone, *Exchange functionals with improved long-range behavior and adiabatic connection methods without adjustable parameters: The mPW and mPW1PW models*, J. Chem. Phys. **108**, 664 (1998), doi:[10.1063/1.475428](https://doi.org/10.1063/1.475428).

- [76] Y. Zhao and D. G. Truhlar, *Hybrid meta density functional theory methods for thermochemistry, thermochemical kinetics, and noncovalent interactions: The MPW1B95 and MPWB1K models and comparative assessments for hydrogen bonding and van der Waals interactions*, J. Phys. Chem. A **108**, 6908 (2004), doi:[10.1021/jp048147q](https://doi.org/10.1021/jp048147q).
- [77] A. J. Cohen and N. C. Handy, *Dynamic correlation*, Mol. Phys. **99**, 607 (2001), doi:[10.1080/00268970010023435](https://doi.org/10.1080/00268970010023435).
- [78] J. P. Perdew, M. Ernzerhof and K. Burke, *Rationale for mixing exact exchange with density functional approximations*, J. Chem. Phys. **105**, 9982 (1996), doi:[10.1063/1.472933](https://doi.org/10.1063/1.472933).
- [79] L. Lu, H. Hu, H. Hou and B. Wang, *An improved B3LYP method in the calculation of organic thermochemistry and reactivity*, Comput. Theor. Chem. **1015**, 64 (2013), doi:[10.1016/j.comptc.2013.04.009](https://doi.org/10.1016/j.comptc.2013.04.009).
- [80] R. Peverati and D. G. Truhlar, *Communication: A global hybrid generalized gradient approximation to the exchange-correlation functional that satisfies the second-order density-gradient constraint and has broad applicability in chemistry*, J. Chem. Phys. **135**, 191102 (2011), doi:[10.1063/1.3663871](https://doi.org/10.1063/1.3663871).
- [81] Y. Zhao, B. J. Lynch and D. G. Truhlar, *Development and assessment of a new hybrid density functional model for thermochemical kinetics*, J. Phys. Chem. A **108**, 2715 (2004), doi:[10.1021/jp049908s](https://doi.org/10.1021/jp049908s).
- [82] Y. Zhao and D. G. Truhlar, *The M06 suite of density functionals for main group thermochemistry, thermochemical kinetics, noncovalent interactions, excited states, and transition elements: two new functionals and systematic testing of four M06-class functionals and 12 other functionals*, Theor. Chem. Acc. **120**, 215 (2007), doi:[10.1007/s00214-007-0310-x](https://doi.org/10.1007/s00214-007-0310-x).
- [83] Y. Zhao and D. G. Truhlar, *Exploring the limit of accuracy of the global hybrid meta density functional for main-group thermochemistry, kinetics, and noncovalent interactions*, J. Chem. Theory Comput. **4**, 1849 (2008), doi:[10.1021/ct800246v](https://doi.org/10.1021/ct800246v).
- [84] R. Peverati and D. G. Truhlar, *Improving the accuracy of hybrid meta-GGA density functionals by range separation*, J. Phys. Chem. Lett. **2**, 2810 (2011), doi:[10.1021/jz201170d](https://doi.org/10.1021/jz201170d).
- [85] H. S. Yu, X. He, S. L. Li and D. G. Truhlar, *MN15: A Kohn-Sham global-hybrid exchange-correlation density functional with broad accuracy for multi-reference and single-reference systems and noncovalent interactions*, Chem. Sci. **7**, 5032 (2016), doi:[10.1039/c6sc00705h](https://doi.org/10.1039/c6sc00705h).
- [86] Y. Zhao and D. G. Truhlar, *Design of density functionals that are broadly accurate for thermochemistry, thermochemical kinetics, and nonbonded interactions*, J. Phys. Chem. A **109**, 5656 (2005), doi:[10.1021/jp050536c](https://doi.org/10.1021/jp050536c).

- [87] G. I. Csonka, J. P. Perdew and A. Ruzsinszky, *Global hybrid functionals: A look at the engine under the hood*, J. Chem. Theory Comput. **6**, 3688 (2010), doi:[10.1021/ct100488v](https://doi.org/10.1021/ct100488v).
- [88] K. Hui and J.-D. Chai, *SCAN-based hybrid and double-hybrid density functionals from models without fitted parameters*, J. Chem. Phys. **144**, 044114 (2016), doi:[10.1063/1.4940734](https://doi.org/10.1063/1.4940734).
- [89] V. N. Staroverov, G. E. Scuseria, J. Tao and J. P. Perdew, *Comparative assessment of a new nonempirical density functional: Molecules and hydrogen-bonded complexes*, J. Chem. Phys. **119**, 12129 (2003), doi:[10.1063/1.1626543](https://doi.org/10.1063/1.1626543).
- [90] T. Yanai, D. P. Tew and N. C. Handy, *A new hybrid exchange-correlation functional using the Coulomb-attenuating method (CAM-B3LYP)*, Chem. Phys. Lett. **393**, 51 (2004), doi:[10.1016/j.cplett.2004.06.011](https://doi.org/10.1016/j.cplett.2004.06.011).
- [91] J. Heyd, G. E. Scuseria and M. Ernzerhof, *Hybrid functionals based on a screened Coulomb potential*, J. Chem. Phys. **118**, 8207 (2003), doi:[10.1063/1.1564060](https://doi.org/10.1063/1.1564060).
- [92] J. Heyd, G. E. Scuseria and M. Ernzerhof, *Erratum: "Hybrid functionals based on a screened Coulomb potential" [J. Chem. Phys. 118, 8207 (2003)]*, J. Chem. Phys. **124**, 124 (2006), doi:[10.1063/1.2204597](https://doi.org/10.1063/1.2204597).
- [93] A. V. Krukau, O. A. Vydrov, A. F. Izmaylov and G. E. Scuseria, *Influence of the exchange screening parameter on the performance of screened hybrid functionals*, J. Chem. Phys. **125**, 224106 (2006), doi:[10.1063/1.2404663](https://doi.org/10.1063/1.2404663).
- [94] J.-D. Chai and M. Head-Gordon, *Long-range corrected hybrid density functionals with damped atom-atom dispersion corrections*, Phys. Chem. Chem. Phys. **10**, 6615 (2008), doi:[10.1039/B810189B](https://doi.org/10.1039/B810189B).
- [95] J.-D. Chai and M. Head-Gordon, *Systematic optimization of long-range corrected hybrid density functionals*, J. Chem. Phys. **128**, 084106 (2008), doi:[10.1063/1.2834918](https://doi.org/10.1063/1.2834918).
- [96] A. Karton, A. Tarnopolsky, J.-F. Lamère, G. C. Schatz and J. M. L. Martin, *Highly accurate first-principles benchmark data sets for the parametrization and validation of density functional and other approximate methods. Derivation of a robust, generally applicable, double-hybrid functional for thermochemistry and thermochemical kinetics*, J. Phys. Chem. A **112**, 12868 (2008), doi:[10.1021/jp801805p](https://doi.org/10.1021/jp801805p).
- [97] S. Grimme, *Semiempirical hybrid density functional with perturbative second-order correlation*, J. Chem. Phys. **124**, 34108 (2006), doi:[10.1063/1.2148954](https://doi.org/10.1063/1.2148954).
- [98] S. Kozuch and J. M. L. Martin, *Spin-component-scaled double hybrids: An extensive search for the best fifth-rung functionals blending DFT and perturbation theory*, J. Comput. Chem. **34**, 2327 (2013), doi:[10.1002/jcc.23391](https://doi.org/10.1002/jcc.23391).

- [99] E. Brémond and C. Adamo, *Seeking for parameter-free double-hybrid functionals: The PBE0-DH model*, J. Chem. Phys. **135**, 24106 (2011), doi:[10.1063/1.3604569](https://doi.org/10.1063/1.3604569).
- [100] L. Goerigk and S. Grimme, *Efficient and accurate double-hybrid-meta-GGA density functionals—evaluation with the extended GMTKN30 database for general main group thermochemistry, kinetics, and noncovalent interactions*, J. Chem. Theory Comput. **7**, 291 (2010), doi:[10.1021/ct100466k](https://doi.org/10.1021/ct100466k).
- [101] S. Grimme, J. Antony, S. Ehrlich and H. Krieg, *A consistent and accurate ab initio parametrization of density functional dispersion correction (DFT-D) for the 94 elements H-Pu*, J. Chem. Phys. **132**, None (2010), doi:[10.1063/1.3382344](https://doi.org/10.1063/1.3382344).
- [102] S. Grimme, S. Ehrlich and L. Goerigk, *Effect of the damping function in dispersion corrected density functional theory*, J. Comput. Chem. **32**, 1456 (2011), doi:[10.1002/jcc.21759](https://doi.org/10.1002/jcc.21759).
- [103] J. G. Brandenburg, C. Bannwarth, A. Hansen and S. Grimme, *B97-3c: A revised low-cost variant of the B97-D density functional method*, J. Chem. Phys. **148**, 064104 (2018), doi:[10.1063/1.5012601](https://doi.org/10.1063/1.5012601).
- [104] S. Grimme, A. Hansen, S. Ehlert and J.-M. Mewes, *r2SCAN-3c: A “Swiss army knife” composite electronic-structure method*, J. Chem. Phys. **154**, 064103 (2021), doi:[10.1063/5.0040021](https://doi.org/10.1063/5.0040021).
- [105] M. Müller, A. Hansen and S. Grimme,  *$\omega$ B97X-3c: A composite range-separated hybrid DFT method with a molecule-optimized polarized valence double- $\zeta$  basis set*, J. Chem. Phys. **158**, 014103 (2023), doi:[10.1063/5.0133026](https://doi.org/10.1063/5.0133026).
- [106] Y. J. Franzke et al., *TURBOMOLE: Today and tomorrow*, J. Chem. Theory Comput. **19**, 6859 (2023), doi:[10.1021/acs.jctc.3c00347](https://doi.org/10.1021/acs.jctc.3c00347).
- [107] *TURBOMOLE V7.8 2023*, <http://www.Turbomole.Com>.
- [108] M. Haasler, T. M. Maier, R. Grotjahn, S. Gückel, A. V. Arbuznikov and M. Kaupp, *A local hybrid functional with wide applicability and good balance between (De)localization and left-right correlation*, J. Chem. Theory Comput. **16**, 5645 (2020), doi:[10.1021/acs.jctc.0c00498](https://doi.org/10.1021/acs.jctc.0c00498).
- [109] M. Haasler, T. M. Maier and M. Kaupp, *Toward a correct treatment of core properties with local hybrid functionals*, J. Comput. Chem. **44**, 2461 (2023), doi:[10.1002/jcc.27211](https://doi.org/10.1002/jcc.27211).
- [110] C. Holzer and Y. J. Franzke, *A local hybrid exchange functional approximation from first principles*, J. Chem. Phys. **157**, 034108 (2022), doi:[10.1063/5.0100439](https://doi.org/10.1063/5.0100439).

- [111] A. Wodyński and M. Kaupp, *Local hybrid functional applicable to weakly and strongly correlated systems*, J. Chem. Theory Comput. **18**, 6111 (2022), doi:[10.1021/acs.jctc.2c00795](https://doi.org/10.1021/acs.jctc.2c00795).
- [112] A. Wodyński, A. V. Arbuznikov and M. Kaupp, *Strong-correlation density functionals made simple*, J. Chem. Phys. **158**, 244117 (2023), doi:[10.1063/5.0153463](https://doi.org/10.1063/5.0153463).
- [113] S. Fürst, M. Haasler, R. Grotjahn and M. Kaupp, *Full implementation, optimization, and evaluation of a range-separated local hybrid functional with wide accuracy for ground and excited states*, J. Chem. Theory Comput. **19**, 488 (2023), doi:[10.1021/acs.jctc.2c00782](https://doi.org/10.1021/acs.jctc.2c00782).
- [114] S. Fürst, M. Kaupp and A. Wodyński, *Range-separated local hybrid functionals with small fractional-charge and fractional-spin errors: Escaping the zero-sum game of DFT functionals*, J. Chem. Theory Comput. **19**, 8639 (2023), doi:[10.1021/acs.jctc.3c00877](https://doi.org/10.1021/acs.jctc.3c00877).